AEROSPACE REPORT NO.
TOR-2021-01076

REACH Historical Data README (v3.0)

February 26, 2021

Timothy B. Guild, T. Paul O'Brien, Alexander J. Boyd, and Joseph E. Mazur
Space Sciences Department
Space Science Applications Laboratory

Prepared for:

Space and Missile Systems Center
United States Space Force
483 N. Aviation Blvd.
El Segundo, CA 90245-2808

Contract No. FA8802-19-C-0001

Authorized by: Defense Systems Group

Acknowledgments

The success of the REACH project is owed to a long line of people who have contributed to it over the many years of development. The REACH hardware team in The Aerospace Corporation's xLab organization included Paul Carranza, Sue Crain, Bill Crain, Andrew Hsu, Brian McCarthy, John McHale, Can Nguyen, Mario Perez, Deb Salvaggio, and Gerrit Sorensen, all critical to designing and fabricating the first 18 of the 32 REACH pods. Millennium Engineering and Integration (MEI) manufactured the remaining 14 pods. Doug Holker was instrumental in nearly all facets of REACH development, outreach, support, endorsement and project management for the entirety of the project's lifetime. The REACH project was led in chronological order by the following USAF Program Managers: Capt Dan Kimmich, Lt Garrett Ellis, Lt Justin Shimasaki, Capt Sean Quintana, Capt Felix Abeyta, Lt Kurt Mann, Maj James Crane, Capt Omar Manning, Lt Zach Morley, Capt Scott Day, Lt Zeesha Braslawsce, and Lt Ryan Francies. This list reflects their ranks at the time of involvement. Recent management is possible through the SMC/Development Corp program office support Pete Cunningham. Data transport is provided by Iridium, L3Harris, and data processing of the Level 0 files is performed by Robin Barnes and supported by Tom Sotirelis and Mike Kelly at the Johns Hopkins Applied Physics Laboratory. Alexa Halford, now of NASA Goddard Space Flight Center, prototyped many higher-level REACH data products and performed intra-calibration of the dosimeters. Edith Mazur produced Figure 3.

Abstract

This document represents the README for the historical REACH data release. It describes the "v3" files produced at The Aerospace Corporation, from March 2017 until December 2019. It includes a brief mission description, describes the features of the collection of dosimeters, discusses data availability throughout the dataset, describes data quality flags, and concludes with a data dictionary. It includes an excerpt of one example file in Appendix A.

Contents

Figures

Tables

1. REACH Mission Overview

The Responsive Environmental Assessment Commercially Hosted (REACH) constellation is collection of 32 small sensors hosted on six orbital planes of the Iridium-Next space vehicles in low earth orbit. Each sensor contains two micro-dosimeters sensitive to the passage of charged particles from the Earth's radiation belts. There are six distinct dosimeter types spread among the 64 individual sensors, which are unique in shielding and electronic threshold. When taken together, this effectively enables a high time-cadence measurement of protons and electrons in six integral energy channels over the entire globe.

This document accompanies the historical REACH data release from the initial constellation build-out. It describes the host spacecraft, REACH sensors, data volume, ephemeris, magnetic regions, data quality flags, and includes a data dictionary. It is specific to version 3 of the REACH data files. There were no prior versions released to the public.

2. REACH Data Description

2.1 Host Vehicles

The REACH sensors are hosted on 32 Iridium-Next space vehicles. They are internally numbered according to their hosted payload numbers, which differ from their Iridium spacecraft numbers. The conversion, along with each host's NORAD ID and the REACH model number is below in Table 1.

Table 1. Vehicle Identities in the REACH Constellation

REACH Vehicle ID	Iridium Vehicle ID	NORAD ID	Pod Model Number
171	158	43571	0
169	153	43078	0
181	160	43569	0
180	171	43929	0
170	156	43576	0
172	159	43578	0
108	133	42955	1
114	110	43481	1
101	102	41920	1
133	117	42808	1
115	107	42960	1
136	132	42961	1
135	126	42809	1
137	119	42959	1
149	164	43577	1
139	137	43076	1
162	147	43480	1
164	152	43479	1
173	165	43572	1
176	150	43257	1
102	113	42803	2
113	121	42812	2
116	108	41924	2
148	131	43079	2
140	122	42957	2
163	149	43250	2
166	180	43922	2
105	106	41917	3
175	168	43924	3
138	134	43075	3
134	125	42964	3
165	145	43253	3

2.2 REACH Pod Flavors

The 32 REACH sensors are identical in housing, mass, and signal processing electronics with each model containing two dosimeters, A and B. However, they come in four models which vary the dosimeter characteristics of each, yielding six distinct dosimeter types, referred to here as “flavors”. The mapping from model to flavor is given in Table 2.

Table 2. REACH Model Number to Flavor Conversion

Model Number	Dosimeter A Flavor	Dosimeter B Flavor
0	X	Z
1	X	W
2	Y	V
3	Y	U

These types differ in shielding and electronic threshold of the dosimeters. Increasing the amount of Al (equivalent) shielding between the sensitive volume of the dosimeter and space serves to exclude particles below a certain energy threshold, yielding roughly integral-in-energy channels. Varying the electronic threshold to which the dosimeter is sensitive can roughly approximate species; protons deposit more energy in the Si dosimeters than electrons. Between all six flavors of REACH sensors, the constellation provides dose behind 5 depths of shielding thickness. REACH includes one flavor (W) insensitive to electrons due to its high electronic threshold, and one flavor (Z) under only a thin foil (~0 mils Al) with a low electronic threshold. An annotated graphic of the 4 models is shown in Figure 1. Each model has two dosimeter slots, A and B. However, depending on the model, each slot includes a distinct flavor of dosimeter, labeled U, V, W, X, Y, or Z. In the graphic, each flavor is annotated with 3 characteristics: the mils of Al-equivalent shielding in black, a preliminary proton energy threshold in red, and a preliminary electron energy threshold in blue.

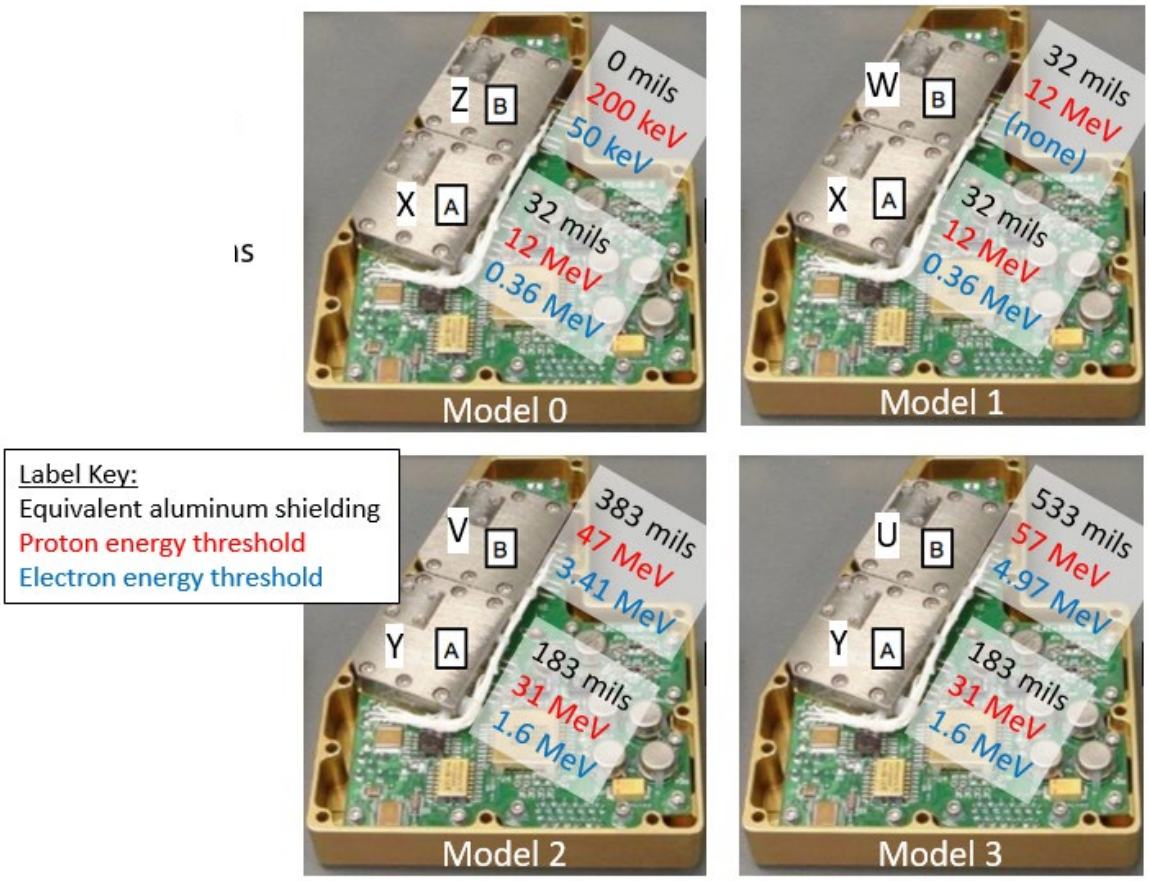

Figure 1. REACH pod model characteristics.

While Figure 1 above provides preliminary dosimeter thresholds, quantitative research should use the flavor characteristics determined from bow-tie analysis of Geant4 response functions determined in O'Brien et al., 2019 [5]. An excerpt of their results is included in Table 3 below for convenience. Flux conversion factors are included in O'Brien et al. 2019 and are used to derive proton and electron fluxes in the REACH data described in this report.

Table 3. REACH Flavor Shielding and Proton/Electron Energy Thresholds Derived from Bow-Tie Analysis

Flavor	Approx. mils Al	Dosimeter Type	Electron Threshold (MeV)	Proton Threshold (MeV)
U	530	MedLET	2.15*	51.5
V	380	MedLET	2.20*	43.9
W	32	HiLET	1.43**	10.5
X	32	MedLET	0.798	12.1
Y	180	MedLET	2.47*	30.3
Z	~0	LoLET	0.0916	1.29

* There are large uncertainties in these electron integral energy thresholds due to the gradual turn-on in the response function to electrons.
**The W flavor responds to electrons with less than 1% the efficiency compared to the X dosimeter.

2.3 Launch Schedule and Data Gaps

The Iridium-Next launch campaign spanned 8 launches from Feb 2017 through March 2019. Each launch delivered 10 space vehicles into one orbit plane and not all the vehicles contained REACH sensors. These sensors have distinct flavors, roughly arranged to attempt to mix flavors into different orbital planes, within the limitations of the REACH integration schedule. This had the effect of increasing the number of REACH sensors providing data throughout the course of the launch campaign, as shown below in Figure 2. The timeseries spans the duration of the dataset included in this release and counts the number of REACH sensors (y-axis) contributing data each day (x-axis) as a function of flavor (colors). These numbers only correspond to the data as it arrived at Aerospace, and for which we have processed data for release. There are episodic data gaps when no data arrived at Aerospace (for example around 07/01/18), and a temporary decrease in the sensors of a given flavor (step down) because of a partial data outage. We make no attempt to fill these gaps here.

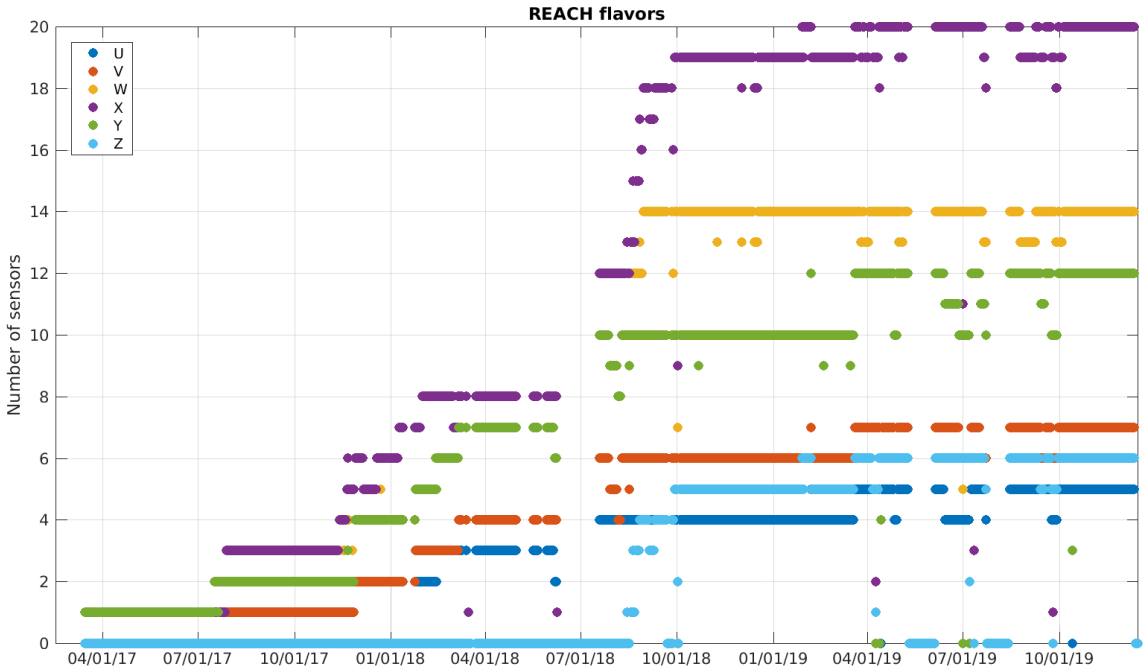

Figure 2. Number of REACH sensor types in the dataset.

A snapshot of the as-populated REACH constellation is shown below in Figure 3. Each orbital plane is color-coded, each marker is labelled with, in order, the Iridium SV number, Hosted Payload number, Plane, slot in plane, and REACH model number of that pod. A map of dose rate is shown in the background. Figure 3 illustrates the global coverage of REACH sensors at a given instant in time.

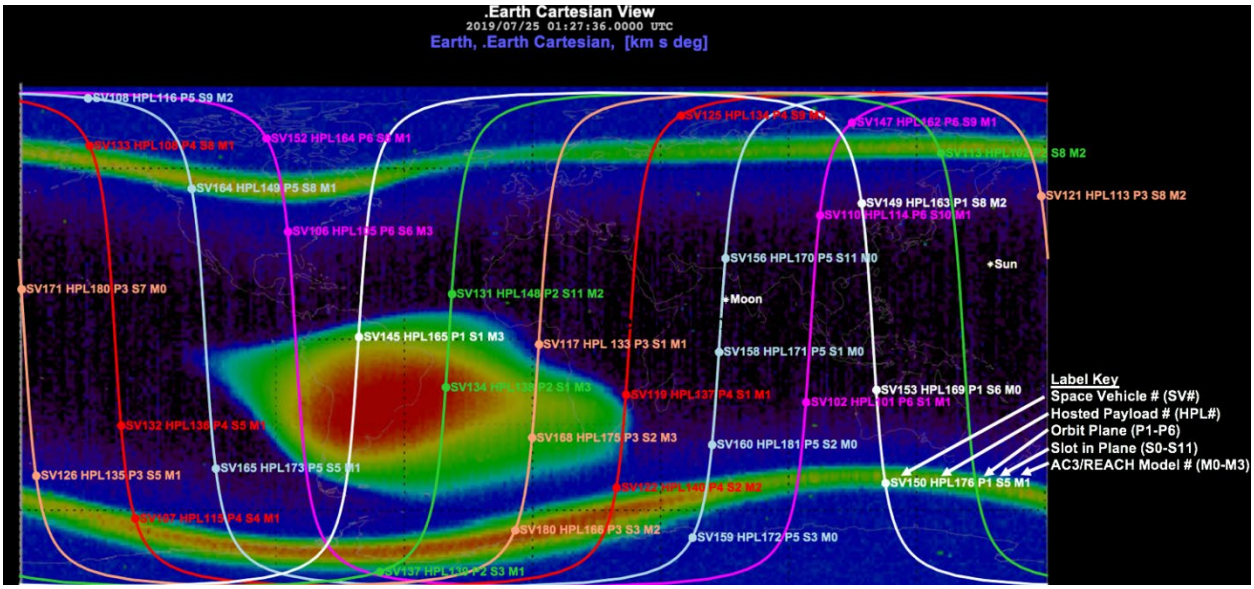

Figure 3. Snapshot of REACH constellation fully populated.

In addition to the data gaps outlined above, the REACH throughput was variable throughout the initial phases of constellation deployment. Receiving less than the expected data from the sensor was likely a function of dropped packets from the space-to-ground link, or in the internet losses during two network hops these packets took between the initial downlink and getting to Aerospace. This throughput was cataloged by counting the number of good 1-second packets received at Aerospace, for each REACH pod, per day. The fractional daily coverage is shown in Figure 4, with each REACH pod displayed in a different color. The top of the y-axis corresponds to the maximum of 24 hours of data per day. Note that only a few REACH pods contribute data early in the launch campaign, with all 32 sensors reporting near the end of Figure 4. Also note the fluctuations in data coverage throughout the launch campaign, when numerous system changes caused both increases, decreases, and gaps in REACH data coverage. The data set begins on 15 March 2017 and ends on 13 December 2019. We make no attempt to fill these coverage shortfalls here.

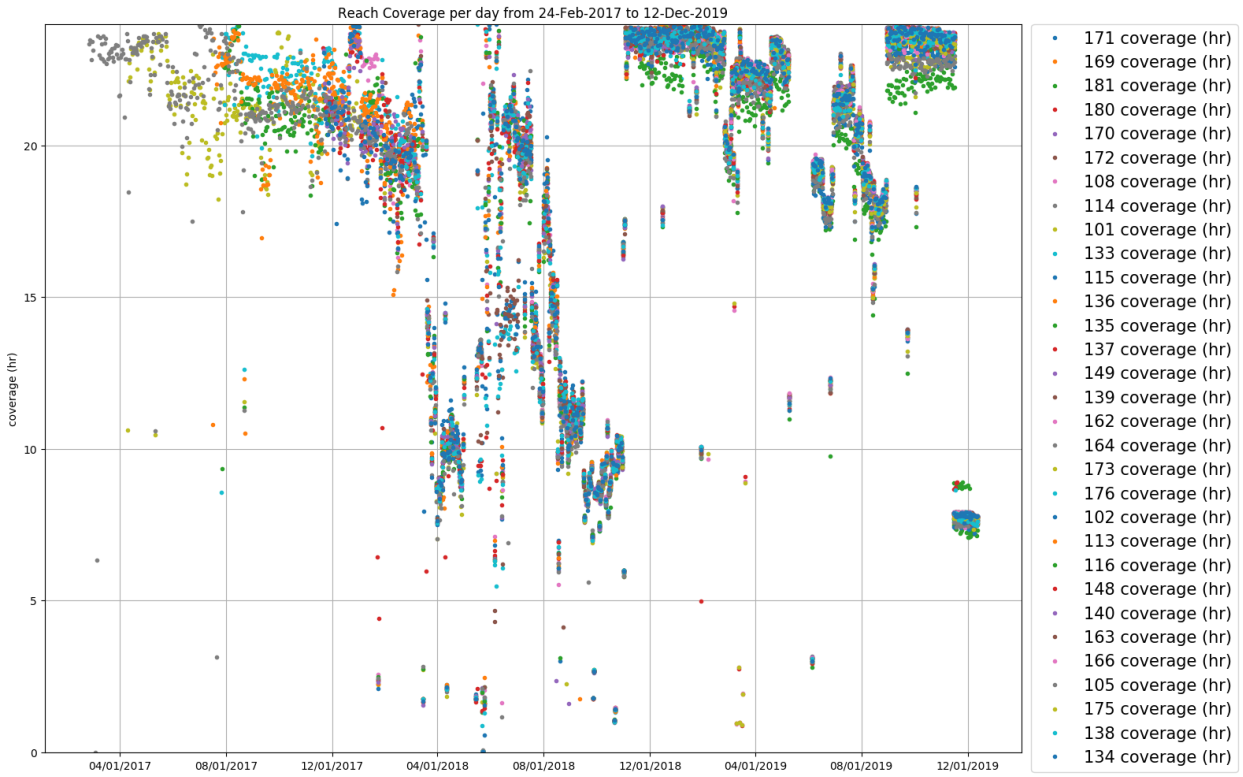

Figure 4. REACH coverage as a function of date.

2.4 Ephemeris and Attitude

The REACH pods are positioned on the nadir deck closest to the ram (forward-facing) side of the Iridium-Next host vehicles. The orientation of the pods is such that the normal direction to the dosimeters is ram and slightly nadir (much like a car headlight directed forward and down to the road ahead). Accordingly, the attitude of the vehicles affects the pitch angle sampling of the REACH sensors. This is most clearly seen when separating the northbound passes from the southbound ones, as shown in Figure 5. The top panel (a) plots the log10(dose rate) in rad/second for the 20 flavor X sensors on 1-Nov-2019 while traveling northbound (orbit status=0). The bottom panel (b) plots the same data while the vehicles are traveling southbound (orbit status = 1). Although qualitatively similar, this pitch angle sampling is seen in a larger south-east extent of the SAA while traveling northbound than while traveling southbound. For example, in the slot (at -40 latitude and 0 longitude) the dose rate is nearly 10x different between the north and southbound passes. At this location the local pitch angle of the sensor normal direction is roughly 15-20 degrees different, leading to this dose rate difference in the strongly peaked pitch angle distribution of the outside edge of the inner zone. This north/southbound flag is provided in the "orbit status" flag in the files described below.

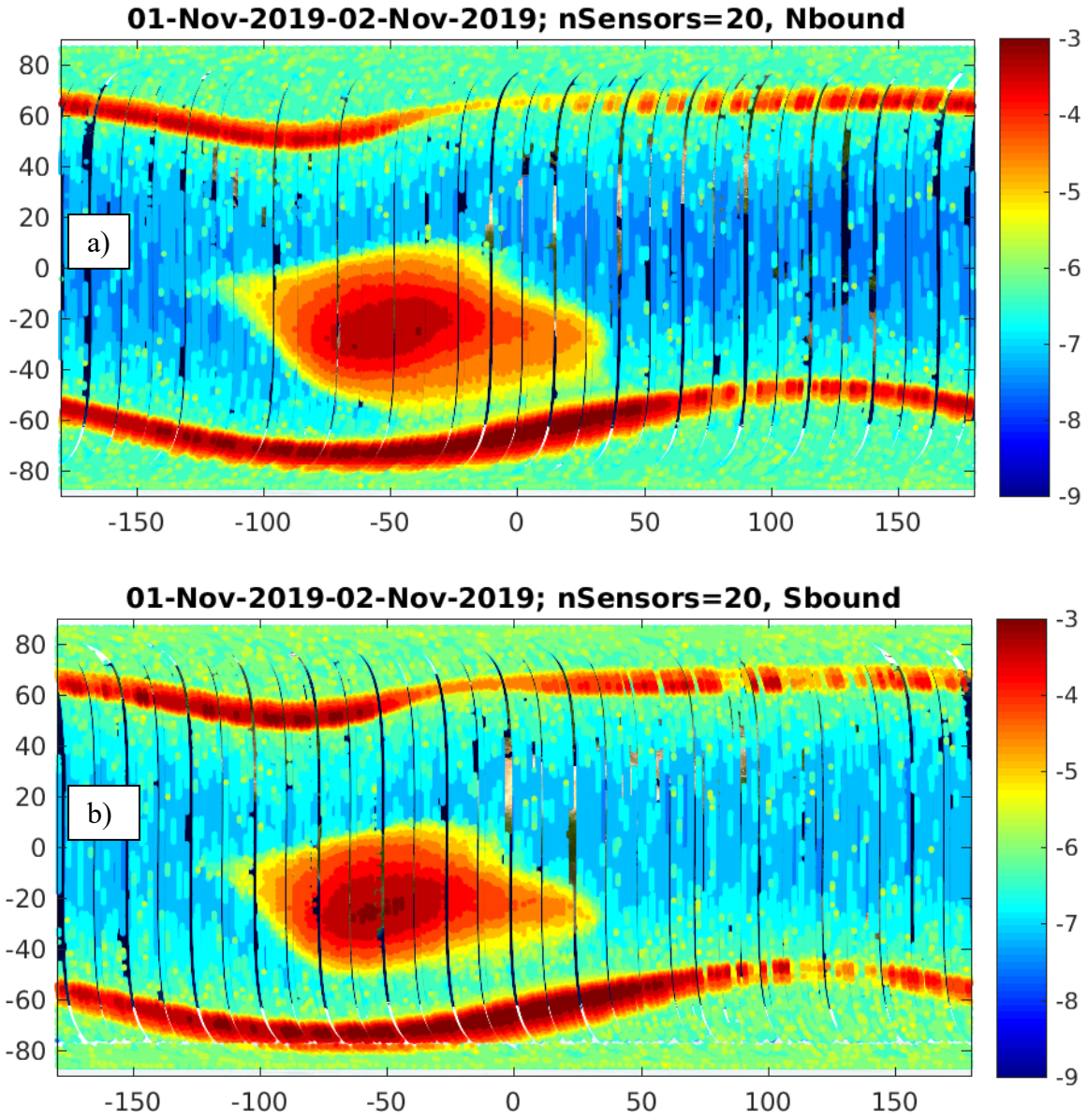

Figure 5. Dose rate from 20 flavor X dosimeters measured while traveling Northbound (a) and Southbound (b). The colorscale is $\log_{10}$(rad/seconds).

2.5 Regions

In order to quickly exploit these data in near-real-time space environment hazard tools, we categorize the position of each REACH sensor into magnetic regions. Regions have been used by NOAA for some time to aggregate POES data into unitless indices which are a proxy for the intensity of the radiation belt population in these regions [4].

The REACH regions were determined from calculating the magnetic coordinates in the IGRF field model at epoch 2018-1-1 00:00 UT at a grid of locations in latitude and longitude at 800 km altitude (roughly the REACH orbit). The regions are defined here in Table 4.

Table 4. Region Code and Description

Region Code	Description and Definition
-4: SPC	Southern Polar cap Lm > 8 or Lm = NaN AND B NOT within 3800 nT of the minimum B in the 0.1 L bin for all points at 800 km.
-3: OZ Untrap	Outer Zone Untrapped. 2.5 <= Lm < 8 AND B NOT within 3800 nT of the minimum B in the 0.1 L bin for all points at 800 km.
-2: Slot Untrap	Slot untrapped. 2 <= Lm <2.5 AND Hmin < 250 km
-1: IZ Untrap	Inner Zone Untrapped. Lm < 2 AND Hmin < 250 km
0: unknown	
+1: IZ Trap	Inner Zone Trapped. Lm < 2 AND Hmin >250 km
+2: Slot Trap	Slot trapped. 2 <= Lm <2.5 AND Hmin < 250 km
+3: OZ trap	Outer Zone Trapped. 2.5 <= Lm < 8 AND B within 3800 nT of the minimum B in the 0.1 L bin for all points at 800 km.
+4: NPC	Southern Polar cap. Lm > 8 or Lm = NaN AND B within 3800 nT of the minimum B in the 0.1 L bin for all points at 800 km.

The logic described above can be understood by coloring the regions on a map, as in Figure 6 below. These region codes are provided in every REACH file (per the data dictionary) in column 40.

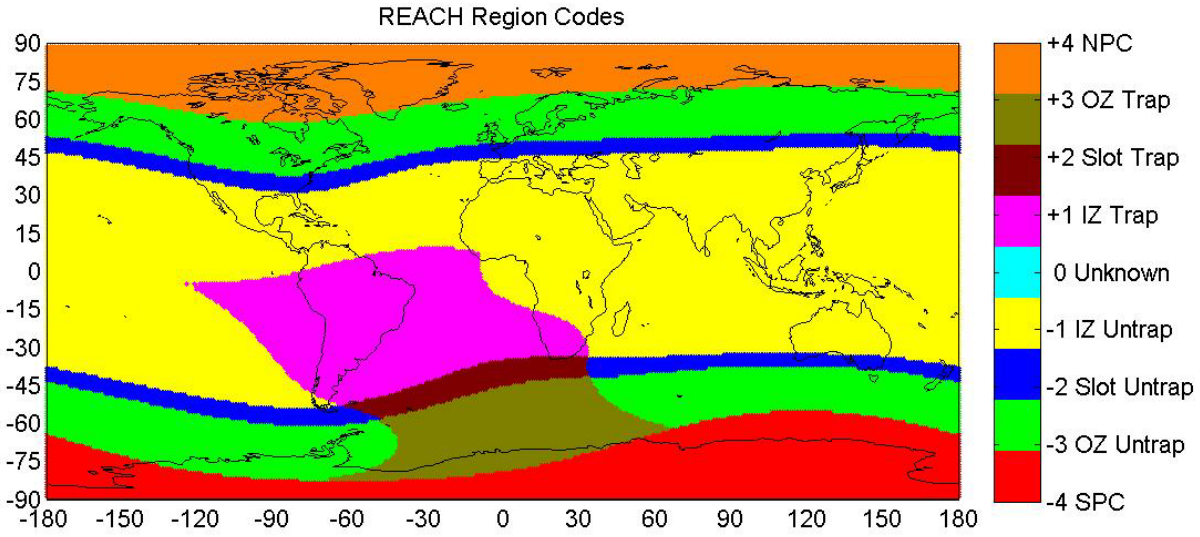

Figure 6. REACH region codes.

2.6 Flags

There are a few nonphysical features in the data which have been identified and flagged so far. After analysis we retain those features in the dataset but identify those times with numbered flags. The flag is a bitmap, or a bitwise "or" of multiple flags which are powers of 2. The flags we have included are related to the sensors being in test mode, dosimeter self-counting if the temperature exceeds a certain threshold, or if we receive duplicate packets. The flag values are:

- -1: no data
- 0: No known problems

- 1: Test Mode
- 2: Possible temperature-related self-counting in Dosimeter A.
- 4: Possible temperature-related self-counting in Dosimeter B.
- 8: Duplicate packets detected.
- 16: Unknown issue with VID 163/Dosimeter B

Temperature: 2 REACH pods (VID 173 and 105) are temperature sensitive and begin to self-count if the payload temperature is larger than a certain value (20º C). If the payload temperature is larger than this threshold, dose rates should be considered contaminated and the data are flagged. No other dosimeters are affected by this flag.

Duplicate packets: An asynchronous communication interface between the REACH pod and the host spacecraft has been shown to lead, sometimes, to a duplicate REACH packet being sent to the spacecraft, while missing the following packet. (e. g. sequence numbers 88, 88, 90). These duplicate packets occur on all REACH payloads, but vids 101, 102, 105 and 135 have consistently more duplicate packets than the other pods as shown in Figure 7.

The duplicate packets have been possibly related to the interaction between the REACH pod and the hosting payload sharing telemetry between missions. The hosting payload from L3Harris is tracking aircraft ADS-B transponders and uses more telemetry while over flight paths. We think this is what leads to the characteristic geographical pattern of the duplicate packets from the most-affected REACH sensors, shown in Figure 8. The majority of worldwide air traffic is found inside the "ribbon" spanning most major landmasses, according to inspection of www.flightradar24.com.

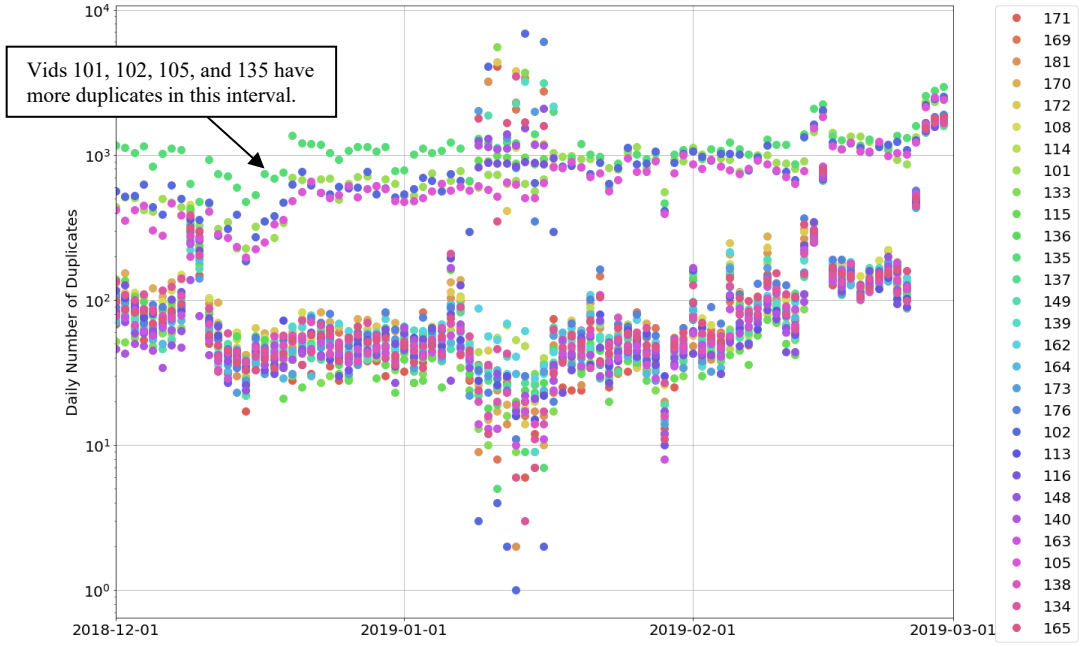

Figure 7. Daily numbers of duplicate packets in REACH pods by date.

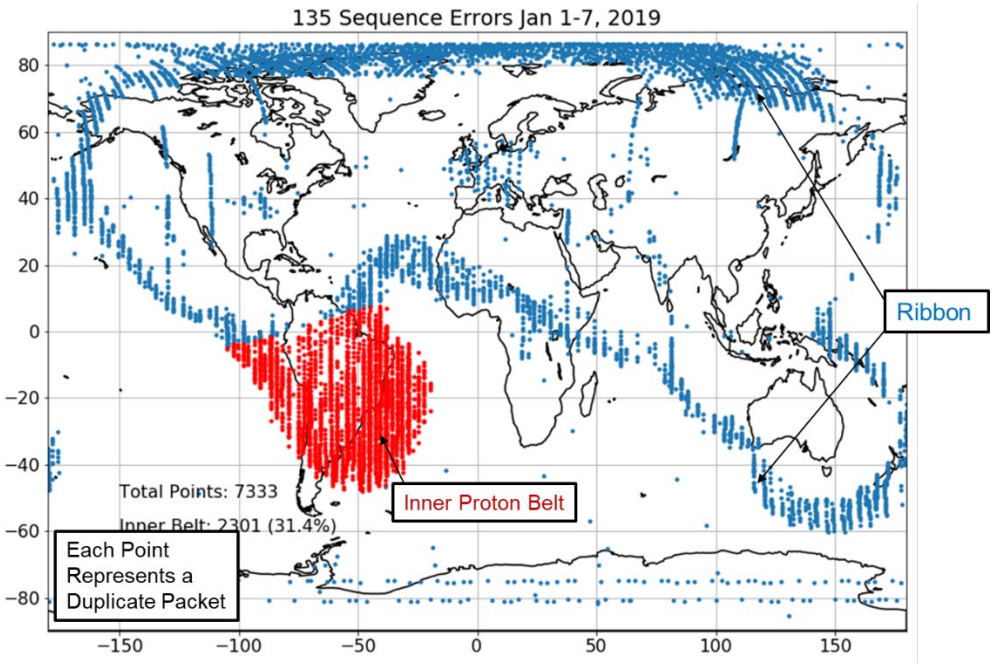

Figure 8. The characteristic pattern of duplicate packets on an affected REACH sensor.

Dosimeter 1 of VID 163 also has an unknown problem with dose rates. Until we investigate it more it will remain flagged all the time.

More careful inspection could yield more than these flags, and we encourage users of the data to be skeptical, and if new features are found please let the instrument team know so we can characterize them and add a new flag to improve the data set in the next version.

2.7 Most Probable Species

Dosimeters cannot unambiguously determine the species of the particle which deposited energy in the silicon detector. However, by analyzing the dose rates of REACH pods in magnetospheric regions which we *a-priori* know the dominant species we can make a guess at the species being measured. This is illustrated in Figure 9 below using the flavor X (electrons > 360 keV, protons > 12 MeV) and W (protons > 12 MeV) pods, which have a common proton energy threshold. Plotting the dose rate versus McIlwain L-shell (Lm), one can clearly distinguish a few features of the radiation belts. For $1 < Lm < 2.4$, the dose rates for both X (e + p) and W (p) are very similar, leading to the conclusion that most of those particles are protons. For the region between $2.4 < Lm < 8$, the W dosimeter is at a "floor" of dose rate corresponding to the low flux of galactic cosmic rays penetrating the magnetosphere. However, flavor X clearly peaks in the Lm range of the outer radiation belt. The dominant species is therefore electrons between 2.4 and 8. Again, for $Lm > 8$ both species are equally present at low dose rates.

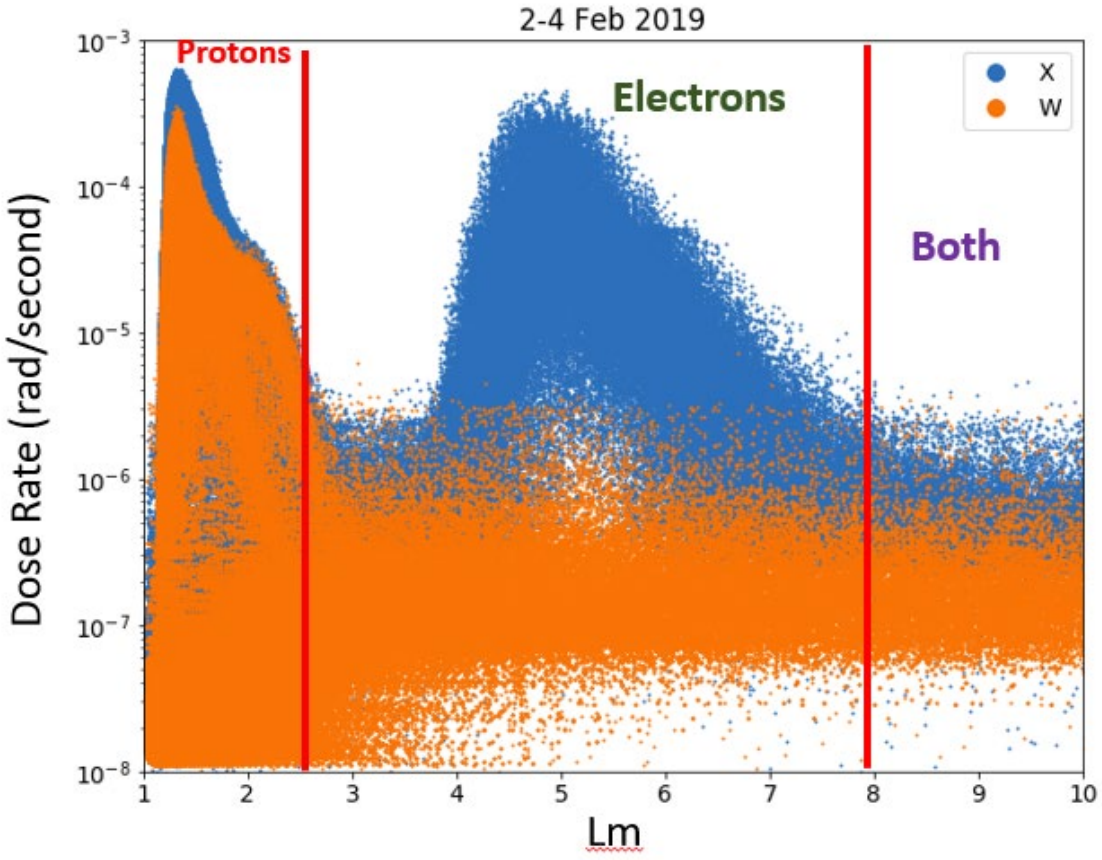

Figure 9. Illustration of the method to identify the most probable species.

An initial survey of all REACH flavors yields the results shown below in Table 5.

Table 5. Locations Corresponding to the Most Probable Species Determinations

Flavor	Protons	Electrons	Both
U	L <3.5, L > 5.5	-	3.5 < L < 5.5
V	L < 3.5, L > 5.5	-	3.5 < L < 5.5
W	All L	-	-
X	L < 2.4	2.4 < L < 8	L > 8
Y	L < 3.5, L > 5.5	-	3.5 < L < 5.5
Z	-	L < 2.1, L > 4.55	2.1 < L < 4.55

In the species columns of the REACH v3 files, a flag is used to describe the most probable species determined in this way. The species flags take the following values: 0 (not currently used), 1 – protons, 2-electrons, and 3-both / ambiguous.

3. REACH Data Dictionary

The REACH data described herein and to be released are considered Level 1b, which means they are processed into rates as a function of time. They include dose rates and fluxes, data quality and best-guess species flags, and geographic and geomagnetic ephemeris.

In Table 6 below, we include the entire data dictionary of the REACH level 1b data. The version covered in this document is "v3". We here cover some basic definitions and notes regarding what is covered in Table 6.

- The bad/missing data value for all fields is –1E31 (-10^{31})
- Dose rate is set to missing data after gap of 3 or more seconds.
- Earth Radius, RE, is 6371.2 km. Geodetic coordinates also use the WGS-84 oblate spheroid.
- Flag is a bitmap (bitwise "or" of multiple flags that are powers of 2). Flag values:
  - -1 – No data
  - 0 – No known problems.
  - 1 – Test Mode
  - 2 – Possible temperature-related self-counting in Dosimeter A.
  - 4 – Possible temperature-related self-counting in Dosimeter B.
  - 8 – Duplicate packets detected.
  - 16 – VID163-Dosimeter A unknown issue.
- GEO – Geographic, Cartesian coordinates. X is through the (0°,0°) latitude longitude point, and Z is through the North geographic pole (Earth's spin axis).
- GEI – Geocentric Earth Inertial. X points to the position of the Sun at the vernal equinox (first point of Aries), and Z is through the North geographic pole (Earth's spin axis).
- IGRF – International Geomagnetic Reference Field [1]
- McIlwain L – McIlwain's magnetic L shell parameter [3]. Also expressed as invariant latitude: $\cos^2\lambda = 1/L$.
- L* (Lstar) – Roederer's magnetic L shell parameter [6]
- K – Kaufmann's modified bounce invariant [2]: We adopt the customary definition of K: $K = \int_{s_m}^{s_{m'}} [B_m - B(s)]^{1/2}\, ds$. The limits of integration are the southern and northern mirror points of the particle's bounce motion, s is the distance along the magnetic field line, B(s) is the magnetic field strength at s, and B_m is the mirror point magnetic field strength.

- α (Alpha) – the angle between a particle's momentum and the magnetic field direction. A locally mirroring particle has α = 90° at the spacecraft.

- α_{eq} (Alpha_Eq) – the angle between a particle's momentum and the magnetic field direction when the particle crosses northward through the weakest point along the magnetic field (the magnetic equator).

- hmin – The minimum mirror altitude around the drift shell for a locally mirroring particle.

- Region Code – See section 2.5

- Orbit Status – See Section 2.4

Table 6. REACH Data Level 1B Dictionary

Column Number	Column	Units	Description
1	MJD	Decimal days	Modified Julian Date
2	YYYY		Year
3	mm		Month
4	DD		Day
5	HH		Hour
6	MM		Minute
7	SEC		Seconds
8	DoY		Day of Year
9	VID		REACH Vehicle Identifier
10	ALT	km	Geodetic Altitude
11	LAT	Degree	Geodetic Latitude
12	LON	degree	Geodetic Longitude
13	GEO_X	Re	GEO coordinates – X
14	GEO_Y	Re	GEO coordinates – Y
15	GEO_Z	Re	GEO coordinates – Z
16	GEI_X	Re	GEI coordinates – X
17	GEI_Y	Re	GEI coordinates – Y
18	GEI_Z	Re	GEI coordinates – Z
19	DOSE1	rad / second	Dose rate from Dosimeter 1
20	PROT FLUX1	#/cm^2/sr/sec	Proton flux from bowtie
21	ELEC FLUX1	#/cm^2/sr/sec	Electron flux from bowtie
22	SPECIES1		Most probable species
23	DOSE2	rad / second	Dose rate from Dosimeter 2
24	PROT FLUX2	#/cm^2/sr/sec	Proton flux from bowtie
25	ELEC FLUX2	#/cm^2/sr/sec	Electron flux from bowtie
26	SPECIES2		Most probable species
27	HK Temperature deg C	deg C	Housekeeping termperature
28	HK 15V Monitor	Volts	Housekeeping voltage
29	HK 5V Monitor	Volts	Housekeeping voltage

Column Number	Column	Units	Description
30	HK 3.3V Monitor	Volts	Housekeeping voltage
31	Lm RE	RE	McIlwain L-shell for locally mirroring particle
32	Inv_Lat deg	Degree	Invariant Latitude for locally mirroring particle
33	Blocal nT	nT	Local magnetic field at s/c
34	Bmin nT	nT	Minimum magnetic field on field line intersecting spacecraft
35	MLT hr	Hour	Magnetic local time
36	K sqrt(G) RE	RE	See above notes
37	hmin km	Km	See above notes
38	Alpha deg	Degree	Local pitch angle
39	Alpha Eq deg	Degree	Equatorial pitch angle
40	Region Code		Described in Section 2.5
41	Orbit Status		1=Northbound, 2=Southbound
42	Flag		Described in Section 2.6

4. References

[1] Finlay, C. C., et al. (2010), "International Geomagnetic Reference Field: The eleventh generation," *Geophys. J. Int.,* **183**(3), 1216-1230, doi:10.1111/j.1365-246X.2010.04804.x.

[2] Kaufmann, R. L., (1965), "Conservation of the first and second adiabatic invariants," *J. Geophys. Res.,* **70**, 2181-6.

[3] McIlwain, C. E. (1961), "Coordinates for mapping the distribution of magnetically trapped particles," J. Geophys. Res., **66**, 3681-91.

[4] NOAA POES radiation belt indices, https://satdat.ngdc.noaa.gov/sem/poes/data/belt_indices/index.html.

[5] O'Brien, T. P., M. D. Looper, J. E. Mazur, REACH Dosimeter Equivalent Energy Thresholds and Flux Conversion Factors, Aerospace Report No. TOR-2019-02016, July 1, 2019.

[6] Roederer, J. G., (1970), *Dynamics of Geomagnetically Trapped Radiation*, Springer-Verlag, New York.

Appendix A. Sample Data File

This appendix includes the first few lines of a REACH l1b version 3 data file from vid-135 on 14 Oct 2019. It serves as an example for all the files, which have the same format, but contain unique data. The data file contains 42 columns, so spans multiple pages below.

Table 7. Sample REACH File for VID-135 for 14 October 2019

MJD	YYYY	mm	DD	HH	MM	SEC	DoY	VID	ALT km	LAT deg	LON deg	GEO_X RE	GEO_Y RE	GEO_Z RE
58770	2019	10	14	0	0	0	287	135	808.06	-85.5933	144.694	-0.07094	0.050236	-1.12122
58770	2019	10	14	0	0	5	287.0001	135	808.07	-85.7581	147.935	-0.07091	0.044422	-1.12147
58770	2019	10	14	0	0	10	287.0001	135	808.078	-85.9082	151.427	-0.07089	0.038607	-1.12168
58770	2019	10	14	0	0	15	287.0002	135	808.086	-86.0418	155.171	-0.07087	0.032791	-1.12187
58770	2019	10	14	0	0	20	287.0002	135	808.092	-86.1572	159.159	-0.07086	0.026975	-1.12202
58770	2019	10	14	0	0	25	287.0003	135	808.097	-86.2528	163.372	-0.07084	0.021157	-1.12215
58770	2019	10	14	0	0	30	287.0003	135	808.1	-86.327	167.781	-0.07083	0.015339	-1.12225
58770	2019	10	14	0	0	35	287.0004	135	808.103	-86.3784	172.344	-0.07082	0.00952	-1.12231
58770	2019	10	14	0	0	40	287.0005	135	808.104	-86.4062	177.008	-0.07081	0.003702	-1.12234
58770	2019	10	14	0	0	45	287.0005	135	808.104	-86.4097	-178.287	-0.07081	-0.00212	-1.12235
58770	2019	10	14	0	0	50	287.0006	135	808.103	-86.389	-173.605	-0.07081	-0.00794	-1.12232
58770	2019	10	14	0	0	55	287.0006	135	808.1	-86.3443	-169.007	-0.07081	-0.01375	-1.12227
58770	2019	10	14	0	1	0	287.0007	135	808.096	-86.2766	-164.548	-0.07081	-0.01957	-1.12218
58770	2019	10	14	0	1	5	287.0008	135	808.091	-86.187	-160.275	-0.07082	-0.02539	-1.12206
58770	2019	10	14	0	1	10	287.0008	135	808.085	-86.0772	-156.219	-0.07082	-0.03121	-1.12192
58770	2019	10	14	0	1	15	287.0009	135	808.078	-85.9487	-152.404	-0.07083	-0.03702	-1.12174
58770	2019	10	14	0	1	20	287.0009	135	808.069	-85.8032	-148.839	-0.07084	-0.04284	-1.12153
58770	2019	10	14	0	1	25	287.001	135	808.059	-85.6425	-145.525	-0.07086	-0.04865	-1.12129
58770	2019	10	14	0	1	30	287.001	135	808.048	-85.4681	-142.458	-0.07087	-0.05447	-1.12102
58770	2019	10	14	0	1	35	287.0011	135	808.036	-85.2817	-139.627	-0.07089	-0.06028	-1.12073
58770	2019	10	14	0	1	40	287.0012	135	808.022	-85.0844	-137.018	-0.07091	-0.06609	-1.1204
58770	2019	10	14	0	1	45	287.0012	135	808.008	-84.8777	-134.616	-0.07094	-0.07189	-1.12004
58770	2019	10	14	0	1	50	287.0013	135	807.992	-84.6626	-132.405	-0.07096	-0.0777	-1.11965
58770	2019	10	14	0	1	55	287.0013	135	807.975	-84.4401	-130.37	-0.07099	-0.0835	-1.11923
...	...	...	...	...	...	...	...	...	...	...	...	...	...	...

GEI_X RE	GEI_Y RE	GEI_Z RE	DOSE1 rad/s	PROT FLUX1 #/cm^2/sr/s	ELEC FLUX1 #/cm^2/sr/s	SPECIES 1	DOSE2 rad/s	PROT FLUX2 #/cm^2/sr/s	ELEC FLUX2 #/cm^2/sr/s	SPECIES 2	HK Temperature deg C	HK 15V Monitor	HK 5V Monitor	HK 3.3V Monitor
-0.08468	0.019613	-1.12122	2.91E-07	0.894218	20.6131	3	7.62E-07	3.49908	8184.14	1	28.0799	14.3555	5	3.28125
-0.08246	0.014212	-1.12147	2.91E-07	0.894218	20.6131	3	7.62E-07	3.49908	8184.14	1	28.0799	14.3555	5	3.28125
-0.08024	0.00881	-1.12168	2.91E-07	0.894218	20.6131	3	7.62E-07	3.49908	8184.14	1	28.0799	14.3555	5	3.28125
-0.07802	0.003408	-1.12187	2.91E-07	0.894218	20.6131	3	7.62E-07	3.49908	8184.14	1	28.0799	14.3555	5	3.28125
-0.07579	-0.00199	-1.12202	2.91E-07	0.894218	20.6131	3	7.62E-07	3.49908	8184.14	1	28.0799	14.3555	5	3.28125
-0.07356	-0.0074	-1.12215	2.91E-07	0.894218	20.6131	3	6.68E-07	3.06502	7168.9	1	28.0799	14.3555	5	3.28125
-0.07133	-0.0128	-1.12225	2.91E-07	0.894218	20.6131	3	5.82E-07	2.6723	6250.34	1	28.0799	14.3555	5	3.28125
-0.0691	-0.0182	-1.12231	2.91E-07	0.894218	20.6131	3	5.82E-07	2.6723	6250.34	1	28.0799	14.3555	5	3.28125
-0.06687	-0.0236	-1.12234	2.91E-07	0.894218	20.6131	3	5.82E-07	2.6723	6250.34	1	28.0799	14.3555	5	3.28125
-0.06463	-0.029	-1.12235	2.91E-07	0.894218	20.6131	3	5.82E-07	2.6723	6250.34	1	28.0799	14.3555	5	3.28125
-0.0624	-0.0344	-1.12232	8.54E-07	2.62118	60.4222	3	5.82E-07	2.6723	6250.34	1	28.0799	14.3555	5	3.28125
-0.06016	-0.0398	-1.12227	2.17E-06	6.65075	153.31	3	5.82E-07	2.6723	6250.34	1	28.0799	14.3555	5	3.28125
-0.05792	-0.0452	-1.12218	1.20E-06	3.68587	84.9649	3	4.82E-07	2.21002	5169.11	1	28.0799	14.3555	5	3.28125
-0.05568	-0.05059	-1.12206	9.20E-07	2.8251	65.1228	3	3.58E-07	1.64502	3847.61	1	28.0799	14.3555	5	3.28125
-0.05343	-0.05599	-1.12192	9.20E-07	2.8251	65.1228	3	3.58E-07	1.64502	3847.61	1	28.0799	14.3555	5	3.28125
-0.05119	-0.06138	-1.12174	7.56E-07	2.32202	53.5261	3	3.58E-07	1.64502	3847.61	1	28.0799	14.3555	5	3.28125
-0.04894	-0.06677	-1.12153	5.56E-07	1.70714	39.3523	3	3.58E-07	1.64502	3847.61	1	28.0799	14.3555	5	3.28125
-0.04669	-0.07216	-1.12129	5.56E-07	1.70714	39.3523	3	3.58E-07	1.64502	3847.61	1	28.0799	14.3555	5	3.28125
-0.04445	-0.07755	-1.12102	5.56E-07	1.70714	39.3523	3	3.58E-07	1.64502	3847.61	1	28.0799	14.3555	5	3.28125
-0.0422	-0.08294	-1.12073	5.56E-07	1.70714	39.3523	3	3.58E-07	1.64502	3847.61	1	28.0799	14.3555	5	3.28125
-0.03994	-0.08832	-1.1204	5.56E-07	1.70714	39.3523	3	3.58E-07	1.64502	3847.61	1	28.0799	14.3555	5	3.28125
-0.03769	-0.0937	-1.12004	4.33E-07	1.32841	30.6219	3	3.58E-07	1.64502	3847.61	1	28.0799	14.3555	5	3.28125
-0.03544	-0.09908	-1.11965	3.97E-07	1.21846	28.0873	3	3.58E-07	1.64502	3847.61	1	28.0799	14.3555	5	3.28125
-0.03318	-0.10446	-1.11923	3.97E-07	1.21846	28.0873	3	3.58E-07	1.64502	3847.61	1	28.0799	14.3555	5	3.28125
…	…	…	…	…	…	…	…	…	…	…	…	…	…	…

Lm RE	Inv_Lat deg	Blocal nT	Bmin nT	MLT hr	K sqrt(G)RE	hmin km	Alpha deg	Alpha Eq deg	Region Code	Orbit Status	Flag
30	-79.5582	39597.8	1.02017	19.7732	51.0218	-1.00E+31	79.0886	0.285564	-4	1	0
29.8446	-79.4526	39611.5	1.0868	19.7238	49.9886	-1.00E+31	79.0343	0.294636	-4	1	0
29.0879	-79.3147	39620.1	1.16356	19.6646	48.6795	-1.00E+31	78.9902	0.304785	-4	1	0
28.1707	-79.1401	39623.7	1.28302	19.591	47.0883	-1.00E+31	79.0443	0.320093	-4	1	0
27.2313	-78.952	39618.3	1.42404	19.5242	45.4532	-1.00E+31	79.1136	0.337327	-4	1	0
26.2784	-78.7509	39603.9	1.58901	19.4646	43.7897	-1.00E+31	79.1962	0.356495	-4	1	0
25.0812	-78.482	39573.5	1.83288	19.3997	41.6939	-1.00E+31	79.389	0.383265	-4	1	0
24.1479	-78.2584	39539.6	2.06148	19.3561	40.0559	-1.00E+31	79.4944	0.406778	-4	1	0
23.028	-77.9721	39485.4	2.39379	19.311	38.0856	-1.00E+31	79.7096	0.438944	-4	1	0
21.8564	-77.649	39418.7	2.78307	19.2765	36.0224	-1.00E+31	79.9316	0.474022	-4	0	0
21.0111	-77.399	39356.7	3.13911	19.2564	34.5298	-1.00E+31	80.0524	0.504015	-4	0	0
20.0372	-77.0912	39269	3.64412	19.2396	32.8057	-1.00E+31	80.2767	0.544022	-4	0	0
19.2326	-76.8192	39191	4.09863	19.2329	31.382	-1.00E+31	80.3942	0.577729	-4	0	0
18.3349	-76.4944	39084.5	4.73266	19.2319	29.7891	-1.00E+31	80.608	0.622043	-4	0	0
17.6918	-76.2464	38992.5	5.29374	19.2371	28.6445	-1.00E+31	80.7122	0.658858	-4	0	0
17.0408	-75.9809	38895	5.90298	19.247	27.487	-1.00E+31	80.8073	0.6968	-4	0	0
16.5986	-75.7915	38818.6	6.39118	19.2578	26.6986	-1.00E+31	80.798	0.725738	-4	0	0
16.2012	-75.6146	38739.5	6.90562	19.2709	25.9877	-1.00E+31	80.7819	0.755117	-4	0	0
15.0115	-75.0427	38785.9	8.68663	19.064	23.9599	-1.00E+31	81.6747	0.84845	-4	0	0
14.7263	-74.8951	38716.2	9.20386	19.0812	23.4477	-1.00E+31	81.5964	0.873956	-4	0	0
14.322	-74.6782	38609.8	10.0113	19.1081	22.7207	-1.00E+31	81.6173	0.912794	-4	0	0
14.0669	-74.5365	38537.6	10.5696	19.1276	22.2616	-1.00E+31	81.5262	0.938561	-4	0	0
13.7019	-74.3266	38427.6	11.435	19.1578	21.6039	-1.00E+31	81.5269	0.977629	-4	0	0
12.6574	-73.6754	38410.5	14.5207	18.993	19.8133	-1.00E+31	82.5027	1.10456	-4	0	0
…	…	…	…	…	…	…	…	…	…	…	…